Journal of The Electrochemical Society, **146** (5) 1707-1711 (1999)
S0013-4651(98)08-022-7 CCC: $7.00 © The Electrochemical Society, Inc.

Cathodic Activity and Interfacial Stability of $Y_{0.8}Ca_{0.2}Co_{1-x}Fe_xO_3$/YSZ Electrodes for Solid Oxide Fuel Cells

Hee Y. Lee, Jong H. Jang, and Seung M. Oh*,z

Division of Chemical Engineering and Institute of Chemical Process, College of Engineering, Seoul National University, Seoul 151-742, Korea

The Fe-doped cobaltates, $Y_{0.8}Ca_{0.2}Co_{1-x}Fe_xO_{3-\delta}$ (x = 0.1-0.7), were prepared and their high-temperature phase stability and cathodic activity were investigated. The perovskite/yttria-stabilized zirconia (YSZ) electrodes were fabricated via a silk printing technique. It was found that the undoped cobaltate (x = 0) is so thermally unstable that the preparation of pure perovskite phase was unsuccessful. The partial Fe-doping to Co (x = 0.1-0.7), however, gave us highly crystalline perovskite powders of an orthorhombic lattice. Among those samples of x = 0.1-0.7, the $Y_{0.8}Ca_{0.2}Co_{0.7}Fe_{0.3}O_{3-\delta}$ showed the best cathodic activity which is superior to $La_{0.9}Sr_{0.1}MnO_3$. The thermal expansion coefficient of this material (10.5×10^{-6} cm/cm-K at 25-1000°C) was very close to that of 8 mol % YSZ (10.8×10^{-6} cm/cm-K). As a result of interfacial reaction between $Y_{0.8}Ca_{0.2}Co_{0.7}Fe_{0.3}O_{3-\delta}$ and YSZ electrolyte, a spinel-type oxide was produced. But the interfacial product formation proceeded mainly during the electrode adhesion period (1200°C) whereas its growth during the cell operation (900-1000°C) was negligible.

Manuscript submitted August 6, 1998; revised manuscript received December 8, 1998.

The compounds $La_{1-x}Sr_xMnO_3$ are widely studied for their possible applications as the cathode materials for SOFC systems.[1] Even though these materials show many desirable cathodic properties, there still remain problems to be solved. One of the shortcomings in Mn perovskites is their reactivity with yttria-stabilized zirconia (YSZ) electrolyte, which produces highly resistive interfacial products such as $La_2Zr_2O_7$ and $SrZrO_3$ during the high-temperature cell operation as well as the electrode adhesion period.[2-4] This new phase formation induces a high cell polarization and thus the cathodic activities gradually deteriorate with prolonged cell operation.

It is known that cobalt-containing perovskites, for example, $La_{1-x}Sr_xCoO_{3-\delta}$, exert a better cathodic activity as compared to the Mn counterparts. However, they have similar problems with respect to high temperature phase stability and interfacial product formation. Furthermore, the thermal expansion mismatch with YSZ is known to be more of a problem.[1]

An inspection of the literature on perovskite electrodes for solid oxide fuel cells (SOFCs) reveals that the extent of interfacial product formation is primarily determined by the activity of the A site element in the ABO_3 formula,[5] whereas the cathodic activity is rather dependent on the nature of the B site element.[6] A deliberate selection of both A and B site elements is thus required to have prospective cathode materials that possess high interfacial stability and cathodic activity. In view of this fact, in this study we chose yttrium as the A site element with the expectation that diffusion of yttrium from the electrode to YSZ layer is discouraged because of the lower concentration gradient between the Y-containing perovskite and YSZ electrolyte. Furthermore, the suspected interfacial product at the Y-containing perovskites/YSZ interface, viz. $Y_2Zr_2O_7$, the Y-counterpart of $La_2Zr_2O_7$, is known to be thermodynamically unstable at high temperature such that the formation of a highly resistive phase may be avoided.[7] To increase the electrical conductivity of this material, 20 mol % of Ca^{2+} was substituted for yttrium since its ionic size is very close to Y^{3+}. As the B site element, we selected Co because Co perovskites generally have higher cathodic activity, presumably due to higher oxide vacancy concentration than other transition metal perovskites.[8] The synthetic experiments performed in this study indicated that the initially projected material, $Y_{0.8}Ca_{0.2}CoO_{3-\delta}$, is thermally unstable, therefore we partially substituted the Co with Fe.

We prepared a series of $Y_{0.8}Ca_{0.2}Co_{1-x}Fe_xO_{3-\delta}$ (x = 0.1-0.7) and their high-temperature phase stability was examined. Cathodic activities of these materials were measured as a function of composition and their activity was compared to the most commonly cited $La_{0.9}Sr_{0.1}MnO_3$. The interfacial products formed at the cobaltate/YSZ interface were identified and their effects on the long-term cathodic performances were also examined. Finally, their thermal expansion coefficients were measured in order to see any mismatch with YSZ.

Experimental

Materials.—$Y_{0.8}Ca_{0.2}Co_{1-x}Fe_xO_{3-\delta}$ (x = 0.1-0.7) was synthesized via Pechini method.[9] For this, aqueous solutions of nitrate of Y, Ca, Fe, and Co were first mixed together in a proper molar ratio to which an excess amount of citric acid (1.2 times of the equivalent) was added. Then, an equimolar amount of ethylene glycol to citric acid was added to the resulting solution. The solution was then heated to complete the polymerization and further heated to make charring. The precursor was crushed and calcined at 850°C for 10 h to obtain powder products. $Co_{2.1}Fe_{0.9}O_4$ was also prepared by the Pechini method. Here, the polymeric precursor was calcined at 800°C for 6 h in air.

Deposition of electrodes.—The perovskite powder was dispersed in turpentine oil and silk printed (400 mesh) on an 8 mol % YSZ disk (diameter = 1.8 cm, thickness = 1 mm). Electrode adhesion was performed at 1200°C for 6 h. As a counter and reference electrode, Pt paste (Ferro no. 4082) was silk printed (100 mesh) on the other side of the disk and sintered at 950°C for 1 h. The apparent area of the working, counter, and reference electrode was 0.22, 1.17, and 0.15 cm^2, respectively. For the electrical contact, a piece of Pt gauze was contacted on the cathode surface and pressed with an alumina tube. For the counter and reference electrode, Pt wires were attached on the electrodes with Pt paste. Details on the cell configuration and experimental setup have been described in previous reports.[4,10]

Electrochemical measurements of cathodic properties.—Electrochemical measurements with regard to the cathodic properties of thin layers of the oxide materials were made with a three-electrode configuration under p_{O_2} = 0.21 atm at 900-1000°C. Only the half-cell characteristics of the cathodes were investigated. The oxygen partial pressure in both sides of the cell was the same. AC impedance measurements were made over the frequency range of 0.05 Hz-100 kHz using an EG&G PARC 173 potentiostat, 276 interface, and 5208 two-phase lock-in analyzer. Deconvolution of the complex impedance spectra was performed with an EG&G PARC 378 electrochemical impedance software.

Characterization of interfacial products.—X-ray diffraction (XRD), scanning electron microscopy (SEM), and energy dispersive spectroscopy (EDS) techniques were utilized to identify the inter-

* Electrochemical Society Active Member.
z E-mail: seungoh@plaza.snu.ac.kr

S0013-4651(98)08-022-7 CCC: $7.00 © The Electrochemical Society, Inc.

facial product. For the SEM and EDS measurement, a reaction couple was prepared with two separate pellets of YSZ and $Y_{0.8}Ca_{0.2}Co_{0.7}Fe_{0.3}O_{3-\delta}$ by an uniaxial pressing at 50 MPa and cold isostatic pressing at 100 MPa, followed by sintering at 1400°C for 2 h, 1200°C for 40 h, and 900°C for 30 h in air. The concentration profiles of yttrium, calcium, zirconium, iron, and cobalt were traced across the interfacial boundary. For the X-ray analysis, the powder mixture of YSZ and $Y_{0.8}Ca_{0.2}Co_{0.7}Fe_{0.3}O_{3-\delta}$ was heat-treated at 1400°C for 2 h.

Results and Discussion

High-temperature phase stability of $Y_{0.8}Ca_{0.2}Co_{1-x}Fe_xO_{3-\delta}$.—Thermal stability of a series of $Y_{0.8}Ca_{0.2}Co_{1-x}Fe_xO_{3-\delta}$ (x = 0.1-0.7) was examined by analyzing the XRD patterns of the heat-treated powders. Figure 1 shows the XRD patterns of the undoped powder sample that was obtained by calcining the corresponding precursor gel at 850°C for 10 h. As shown, the undoped sample contains, in addition to the orthorhombic perovskite phase, impurity phases such as Y_2O_3 and Co_3O_4. After a heat-treatment at 1200°C for 6 h, which is the normal condition for electrode adhesion in this study, the phase is completely decomposed to the individual binary oxides. However, the binary oxides recombine to form the perovskite phase when they are heat-treated at 900°C for 30 h. In the last XRD pattern, the peaks arising from the impurity phases are still detected.

In order to improve the thermal stability of Co perovskites, the solid solutions made by Fe-doping (10-70 mol %) were prepared and their thermal stability was examined. A typical example of thermal stability improvement is demonstrated with the 30 mol % Fe-doped cobaltate (Fig. 2). As seen, the calcined powder shows the orthorhombic-type perovskite lattice without discernable impurity phases. The lattice does not collapse even after a heat-treatment at a higher temperature. Steele et al.[8] reported that thermal stability of perovskite compounds depends on the type of B site element with the following decreasing order: $Fe^{3+} > Mn^{3+} > Co^{3+}$. There they explained this feature based on the fact that Fe–O bond energy is higher than Co–O bond energy. The observed thermal stability improvement by Fe-doping can thus be explained with the same reasoning. The XRD patterns were indexed using an orthorhombic lattice with the lattice constants of a = 5.24 Å, b = 5.49 Å, and c = 7.53 Å (Table I).

Cathodic activities of $Y_{0.8}Ca_{0.2}Co_{1-x}Fe_xO_{3-\delta}$.—Cathodic activities of $Y_{0.8}Ca_{0.2}Co_{1-x}Fe_xO_{3-\delta}$ were compared by recording their steady-state polarization curves (Fig. 3). The same measurement was made with $La_{0.9}Sr_{0.1}MnO_3$, and its activity was compared to the cobaltates. Among the cobaltates, the 30 mol % Fe-doped cobaltate showed the best cathodic activity, which is higher than the manganite. Both the Co-rich perovskites (x < 0.3) and Fe-rich ones (x > 0.3) exhibited a poorer activity than this material. This composition-dependent activity of $Y_{0.8}Ca_{0.2}Co_{1-x}Fe_xO_{3-\delta}$ may be explained as follows. It is generally accepted that Co perovskites possess a higher amount of oxide vacancy than the Fe counterparts because Co–O bond strength is weaker than Fe–O bond. A higher oxide ion conductivity is thus expected in the former.[6,8] It has been proposed that, with a higher oxide ion conductivity, the O_2 reduction reaction in Co perovskites takes place on the electrode surface in addition to the three-phase boundary sites such that a higher current can be delivered. In this sense, it is expected that the best activity can be obtained with the undoped cobaltate in this study. By contrast, the weaker Co–O bond gives rise to a poorer thermal stability for this material. It is thus likely in this study that the Co-rich electrodes (x < 0.3) do not show the desirable activity due to the impurity phases, whereas the Fe-enriched ones (x > 0.3) are not so good due to the intrinsically poorer activity of Fe perovskites, which stems from the stronger Fe–O bond, lower

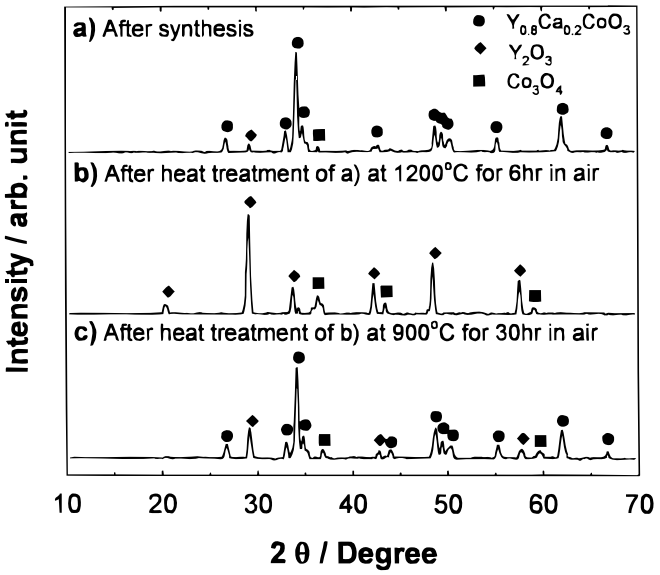

Figure 1. XRD observed with $Y_{0.8}Ca_{0.2}CoO_{3-\delta}$ powder (x = 0.0) according to heat-treatment conditions.

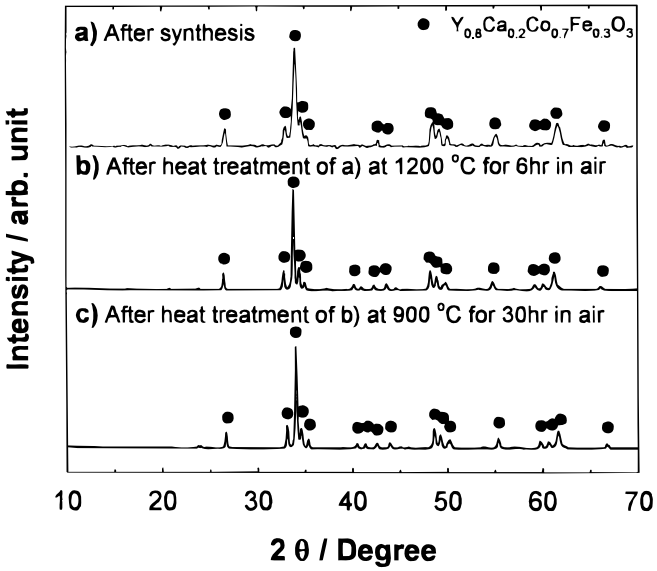

Figure 2. XRD observed with $Y_{0.8}Ca_{0.2}Co_{0.7}Fe_{0.3}O_{3-\delta}$ powder (x = 0.3) according to the heat-treatment conditions.

Table I. X-ray diffraction data for $Y_{0.8}Ca_{0.2}Co_{0.7}Fe_{0.3}O_3$.

2θ	*d*	*hkl*
23.6	3.76	002
26.3	3.39	111
32.6	2.75	020
33.6	2.67	112
34.2	2.62	200
34.8	2.58	021
40.0	2.25	022
40.8	2.21	202
42.1	2.14	113
43.4	2.08	122
48.1	1.89	220
48.7	1.87	221
49.6	1.84	023
54.6	1.68	114,131
59.0	1.56	132
59.9	1.54	024
61.0	1.52	312
65.9	1.42	224

a = 5.24 (Å), b = 5.49 (Å), c = 7.53 (Å).

S0013-4651(98)08-022-7 CCC: $7.00 © The Electrochemical Society, Inc.

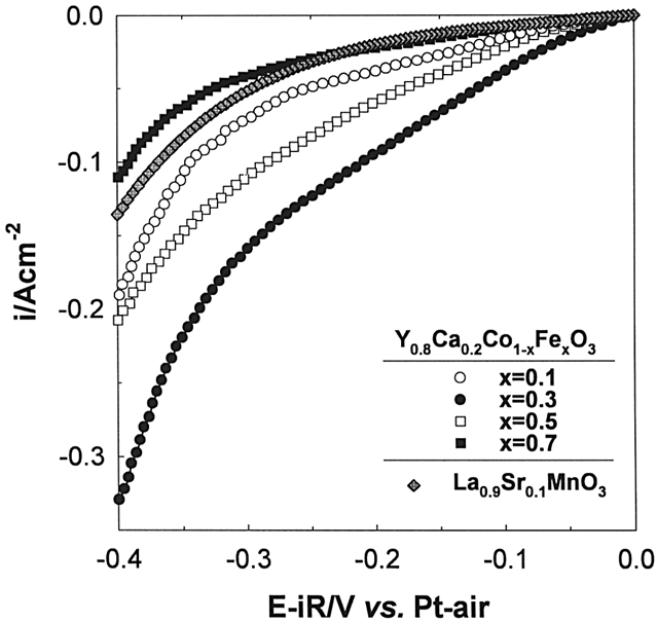

Figure 3. Steady-state polarization curves measured with $Y_{0.8}Ca_{0.2}Co_{1-x}Fe_xO_{3-\delta}$ (x = 0.1-0.7) at 900°C in air. For a comparison, the result obtained with $La_{0.9}Sr_{0.1}MnO_3$ is provided.

oxide vacancy content, and lower oxide ion conductivity. The best trade-off between the two conflicting parameters, the cathodic activity and thermal stability, seems to be made at $x = 0.3$.

Interfacial reaction products.—Figure 4a shows the ac impedance spectra obtained with the $x = 0.3$ electrode. In Fig. 4b, a deconvoluted spectrum and the equivalent circuit used to fit the spectra are presented. The best deconvolution was achieved with the equivalent circuit $R_1(R_2Q_2)(R_3Q_3)(R_4Q_4)$.[11,12] Here, the R_1 was assigned to the ohmic resistance of the electrolyte. The R_2Q_2 was accounted for with the parallel combination of the resistance and constant-phase element (CPE)[12] for the oxide conduction through the electrode, based on the finding that a thicker electrode gave a higher resistance value. The R_3Q_3 was assigned to the parallel combination of the resistance ($R_{interface}$) and the CPE of the interfacial product layer[4] that was formed during the electrode adhesion period, based on the observation that this component grew significantly when the adhesion temperature became higher (>1300°C). The remaining R_4Q_4 component was accounted for with the charge-transfer resistance (R_{ct}) for the O_2 reduction reaction and the corresponding CPE as the semicircles for this component were p_{O_2}-dependent.[4] The deconvoluted R_3 ($R_{interface}$) and R_4 (R_{ct}) values are plotted against the operating time in Fig. 5, where the results obtained with $La_{0.9}Sr_{0.1}MnO_3$ are also displayed.

A comparison of the resistance values obtained with the two electrodes shows that the Fe-doped cobaltate ($x = 0.3$) has two advantageous features as compared to the manganite. The $x = 0.3$ electrode exhibits smaller values in both the charge-transfer resistance (R_4) and the resistance arising from the interfacial product layer (R_3). In addition, even though the R_3 for the manganite steadily increases with cell operation due to the growth of an interfacial product layer, those for the $x = 0.3$ electrode do not increase, indicating that the reaction product at the cobaltate/YSZ interface, whatever its nature, does not grow during the cell operation at 900°C. The same negligible increase in R_3 was observed at 1000°C. It is concluded from this

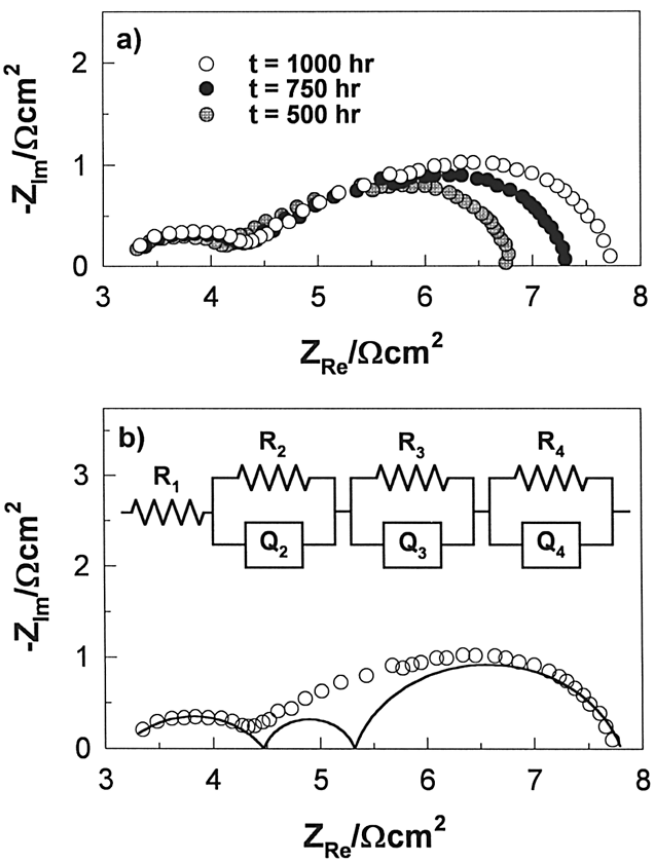

Figure 4. (a) Evolution of ac impedance spectra recorded at 900°C in air as a function of operation time and (b) deconvoluted impedance spectrum (solid line) with the equivalent circuit indicated in the inset.

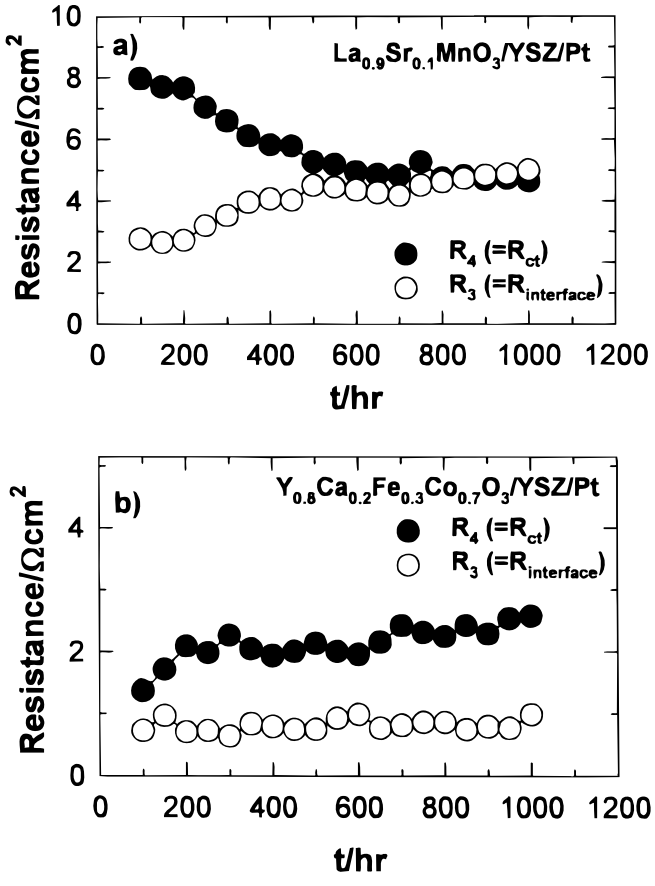

Figure 5. Plots of charge-transfer resistance (R_4) and resistance due to interfacial reaction layer (R_3) as a function of operation time at 900°C in air: (a) $La_{0.9}Sr_{0.1}MnO_3$/YSZ/Pt cell and (b) $Y_{0.8}Ca_{0.2}Co_{0.7}Fe_{0.3}O_{3-\delta}$/YSZ/Pt cell.

S0013-4651(98)08-022-7 CCC: $7.00 © The Electrochemical Society, Inc.

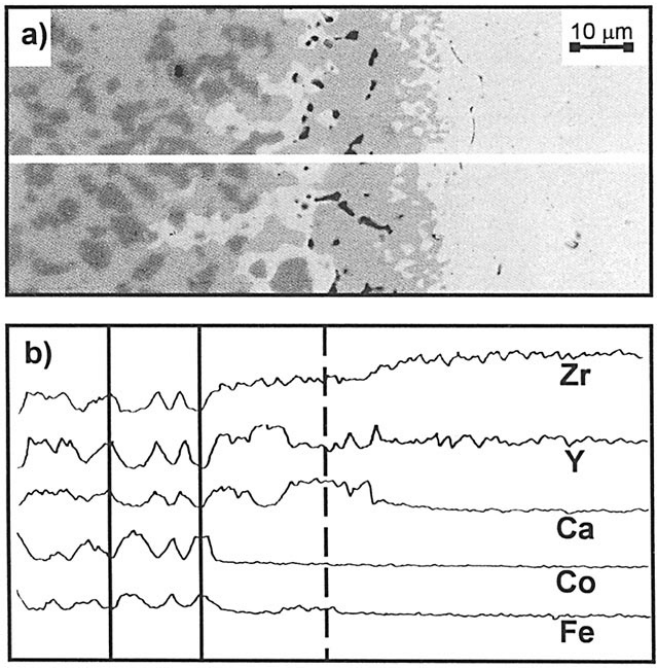

Figure 6. (a) SEM photograph scanned over the interfacial region of $Y_{0.8}Ca_{0.2}Co_{0.7}Fe_{0.3}O_{3-\delta}$ /YSZ and (b) EDS concentration profiles of the constituent elements along the line shown in (a). In (b) the left solid line corresponds to the light spot and the right solid line to the dark spot. The dashed line indicates the boundary between $Y_{0.8}Ca_{0.2}Co_{0.7}Fe_{0.3}O_{3-\delta}$ (left side) and YSZ (right side).

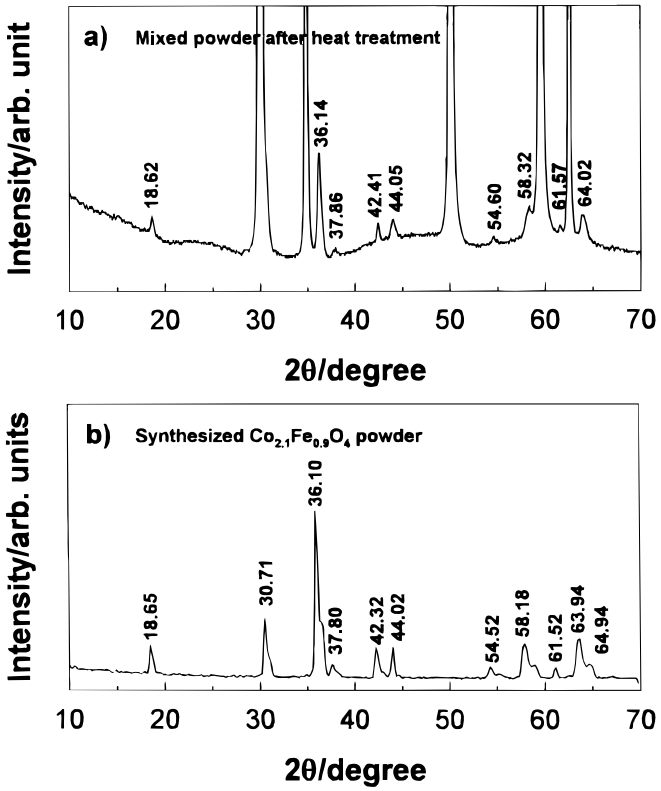

Figure 7. (a) X-ray diffraction pattern recorded after a heat-treatment (1400°C for 2 h) of the powder mixture (YSZ: $Y_{0.8}Ca_{0.2}Co_{0.7}Fe_{0.3}O_{3-\delta}$ = 10:1 weight ratio) and (b) X-ray diffraction pattern of the separately synthesized $Co_{2.1}Fe_{0.9}O_4$ powder. In (a) the unindexed diffraction peaks belong to zirconia and the perovskite.

observation that the interfacial product is formed during the electrode adhesion period (1200°C for 6 h) but its growth at the cell operation temperature is negligible. The interfacial stability of $La_{0.9}Sr_{0.1}MnO_3$ with YSZ electrolyte has been investigated in this and other laboratories.[2-4] It has been found that a pyrochlore-type $La_2Zr_2O_7$ is formed at the interface, and this grows during the cell operation (900-1000°C) as well as the electrode adhesion period.

To identify the nature of interfacial products formed at the $Y_{0.8}Ca_{0.2}Co_{0.7}Fe_{0.3}O_{3-\delta}$/YSZ, the reaction couple made with pressure-contacted sintered pellets of YSZ and perovskite was heat-treated and the interfacial region was analyzed with SEM and EDS techniques (Fig. 6). The SEM picture illustrates that there are dark and light domains dispersed in the electrode side (the left in the picture). The EDS profiles traced along the white line shown in Fig. 6a indicate that the A site ions, more significantly Ca ions, move to the interfacial boundary (the dotted line) and appreciable amounts of Zr ions are counter-diffused from the electrolyte to the electrode side. It is also evident that Co and Fe ions show a maximum population at the dark spots where in turn the population of Ca, Y, and Zr ions is at a minimum. By contrast, Co and Fe ions are depleted at the light spots where Ca, Y, and Zr ions are enriched. This observation leads us to infer that there is a phase separation in the perovskite layer so as to generate Co- and Fe-rich oxides (dark spots), and Y-, Ca-, and Zr-rich oxides (light ones). The former was identified as $Co_{2.1}Fe_{0.9}O_4$ as described below and the latter as the fluorite phases (ZrO_2) containing Ca and Y ions.

Figure 7 shows the XRD pattern recorded after a heat-treatment of the powder mixture (YSZ: $Y_{0.8}Ca_{0.2}Co_{0.7}Fe_{0.3}O_{3-\delta}$ = 10:1 in weight ratio), where additional diffraction peaks as well as those of YSZ and the perovskite can clearly be identified. In Fig. 7a, only the newly developed diffraction peaks are indexed and the unindexed ones belong to zirconia and the perovskite. Based on the fact that the dark spots in Fig. 6a are Fe and Co enriched and the atomic ratio of Co:Fe is 7:3 in the electrode material, a spinel-type $Co_{2.1}Fe_{0.9}O_4$ was proposed as the interfacial product. To ascertain this, the powder of $Co_{2.1}Fe_{0.9}O_4$ was separately synthesized via the Pechini method and its X-ray powder pattern was traced (Fig. 7b). The peak position in the latter pattern is well matched with those of the newly developed one in Fig. 7a. The formation of Ca- and Y-stabilized ZrO_2 was also proposed in this study after the interfacial reaction (the light spots in Fig. 6), but its diffraction lines cannot be indexed in Fig. 7a because of the closeness in the diffraction angles between YSZ and Ca/Y-stabilized zirconia. In Fig 7a, the diffraction lines belonging to the perovskite phase were not isolated also, because the perovskite content was low in the powder mixture. Furthermore, even the most intense diffraction peak (two theta = 34.2) is superimposed with one of the zirconia peaks (see Fig. 2 and Fig. 7a).

Thermal expansion coefficient of $Y_{0.8}Ca_{0.2}Co_{0.7}Fe_{0.3}O_{3-\delta}$.—As mentioned in the introductory section, cobalt-containing perovskites including $La_{1-x}Sr_xCoO_{3-\delta}$ are not highly evaluated as the prospective cathode materials for SOFC applications due to their thermal expansion mismatch with YSZ. The thermal expansion coefficient of the newly prepared $Y_{0.8}Ca_{0.2}Co_{0.7}Fe_{0.3}O_{3-\delta}$ was measured in the temperature range of 25-1000°C in air (Fig. 8). As presented, the thermal expansion coefficient of this material is 10.5×10^{-6} cm/cm-K which is very close to that of YSZ (10.8×10^{-6} cm/cm-K).[13]

Conclusion

The Fe-doped cobaltates, $Y_{0.8}Ca_{0.2}Co_{1-x}Fe_xO_{3-\delta}$ (x = 0.1-0.7), were prepared and their cathodic properties such as the oxygen reduction activity, interfacial stability against YSZ, and thermal expansion mismatch with YSZ were examined. The following points are of value to note.

1. The preparation of undoped cobaltate (x = 0.0) was unsuccessful because of its poor thermal stability at high temperature. The partial substitution of Co with Fe, however, greatly improved the thermal stability of the electrode materials. The cobaltates have an orthorhombic 1attice.

S0013-4651(98)08-022-7 CCC: $7.00 © The Electrochemical Society, Inc.

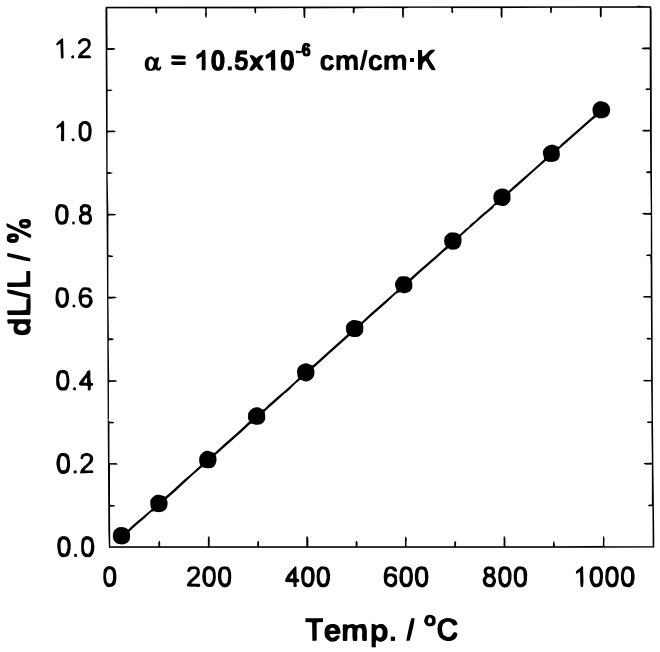

Figure 8. Linear thermal expansion coefficient of $Y_{0.8}Ca_{0.2}Co_{0.7}Fe_{0.3}O_{3-\delta}$ pellet. Density of the sintered pellet was 92% of the theoretical value. Heating rate was 5°C/min.

2. In the series of cobaltates $x = 0.1$-0.7, the 30 mol % Fe-doped one showed the best cathodic activity which is superior to $La_{0.9}Sr_{0.1}MnO_3$.

3. At the interface with YSZ, a spinel-type $Co_{2.1}Fe_{0.9}O_4$ was produced. Its formation mainly took place during the electrode adhesion period (1200°C) whereas its growth rate was negligible at the cell operation temperature (900-1000°C). This behavior is contrasted with $La_{0.9}Sr_{0.1}MnO_3$, where the interfacial product ($La_2Zr_2O_7$) is steadily grown at 900-1000°C as well as the electrode adhesion temperature.

4. The thermal expansion coefficient of $x = 0.3$ sample was very close to that of YSZ. It is thus expected that an electrode failure caused by a thermal shock is not significant with this electrode material.

Finally, the superior cathodic activity of the present materials as compared to $La_{0.9}Sr_{0.1}MnO_3$ and the best activity with $x = 0.3$ electrode has been ascribed to the mixed-conducting behavior of the materials. To confirm this, detailed studies on the oxide vacancy concentration and oxide ion conductivity should be made as a function of Fe substitution. A forthcoming paper will deal with this subject.[14]

Acknowledgment

This work was supported by Ssangyong Cement Industry and Korea Science and Engineering Foundation (966-0304-005-2).

References

1. N. Q. Minh and T. Takahashi, in *Science and Technology of Ceramic Fuel Cells*, p. 118, Elsevier Science, Amsterdam (1995).
2. F. W. Poulsen and N. van der Puil, *Solid State Ionics*, **53-56**, 777 (1992).
3. J. A. M. van Roosmalen and E. H. P. Cordfunke, *Solid State Ionics*, **52**, 303 (1992).
4. H. Y. Lee and S. M. Oh, *Solid State Ionics*, **90**, 133 (1996).
5. H. Yokokawa, N. Sakai, T. Kawada, and M. Dokiya, *Denki Kagaku*, **58**, 489 (1990).
6. Y. Takeda, R. Kanno, M. Noda, Y. Tomida, and O. Yamamoto, *J. Electrochem. Soc.*, **134**, 2656 (1987).
7. D. K. Smith, *J. Am. Ceram. Soc.*, **49**, 625 (1966).
8. S. Carter, A. Selcuk, R. J. Chater, J. Kajda, J. A. Kilner, and B. C. H. Steele, *Solid State Ionics*, **53-56**, 597 (1992).
9. M. P. Pechini, U.S. Pat. 3,330,697 (1967).
10. H. Y. Lee, W. S. Cho, S. M. Oh, H.-D. Wiemhöfer, and W. Göpel, *J. Electrochem. Soc.*, **142**, 2659 (1995).
11. B. A. Boukamp, *Equivalent Circuit*, University of Twente, The Netherlands (1989).
12. J. R. Macdonald and W. B. Johnson, in *Impedance Spectroscopy Emphasizing Solid Materials and Systems*, J. R. Macdonald, Editor, John Wiley & Sons, Inc., New York (1987).
13. N. Q. Minh and T. Takahashi, in *Science and Technology of Ceramic Fuel Cells*, p. 88, Elsevier, Amsterdam (1995).
14. U. Nigge, J. H. Ryu, H.-D. Wiemhöfer, and S. M. Oh, To be published.